$$\mathrm{TCB} - \mathrm{TCG} = \mathrm{c}^{-2}\left\{ \int_{\mathrm{t_0}}^{\mathrm{t}} \left[\frac{\mathrm{v_e^2}}{2} + \mathrm{U_{ext}}\,(\vec{x}_{\mathrm{e}}) \right] \mathrm{dt} + \vec{v}_{\mathrm{e}}.(\vec{x} - \vec{x}_{\mathrm{e}}) \right\} + O(c^{-4}) \tag{2.17}$$

where $\vec{x}_e$ and $\vec{v}_e$ are the barycentric position and velocity of the geocenter, the $\vec{x}$ is the barycentric position of the observer and U_{ext} is the Newtonian potential of all of the solar system bodies apart from the Earth, evaluated at the geocenter. In this formula, t is TCB and t_0 is chosen to be consistent with 1977 January 1, 00h 00m 00s TAI. The neglected terms, $O(c^{-4})$, are of order 10^{-16} in rate for terrestrial observers. $U_{ext}\,(\vec{x}_e)$ and $\vec{v}_e$ are all ephemeris-dependent, and so the resulting TCB belongs to that particular ephemeris, and the term $\vec{v}_e.(\vec{x}$ - $\vec{x}_e)$ is zero at the geocenter.

The all above set of Equations 2.15-2.17 are precisely modeled in INPOP. The numerical integration has been performed to obtain a realization of Equation 2.17 with a nanosecond accuracy (Fienga et al., 2009). The difference between TT-TDB therefore can be extracted at any time from the INPOP planetary ephemeris using the tool called calceph[4]. The spacecraft orbit determination software GINS (see Section 2.5), integrates the equations of motion in the specific coordinate time called, ephemeris time (ET). In GINS, this time is also referred to as TDB, as defined by Moyer (2003). As discrepancies between TT and TDB or ET are smaller than 2 ms (see panel *b* of Figure 2.11), the transformation between the time scales defined either in INPOP or GINS are analogous and show consistency between both software.

2.4.2 Light time solution

The light time solution is used to compute the one-way or round-trip light time of the signal propagating between the tracking station on the Earth and the spacecraft. In order to compute the Doppler and range observables, the first step is to obtain the light time solution. This solution can be modeled by computing the positions and velocities of the transmitter at the transmitting time $t_1(TDB)$, spacecraft at the bouncing time $t_2(TDB)$ (for round-trip) or transmitting time $t_2(TDB)$ (for one-way), and receiver at the receiving time $t_3(TDB)$.

For round-trip light time, spacecraft observations involve two tracking stations, a transmitter, and a receiver which may not be at the same location. Therefore, two light time solutions must be computed, one for up-leg of the signal (transmitter to spacecraft) and one for down-leg (spacecraft to receiver). However, one-way light time requires only single solution because the signal is transmitting by the spacecraft to the receiver. These solutions can be obtained in the Solar system barycenter space-time reference frame for a spacecraft located anywhere in the Solar system.

Since spacecraft observations are usually given at receiver time UTC (see section 2.3.1), the computation sequence therefore works backward in time: given the receiver time $t_3(UTC)$,

[4] http://www.imcce.fr/inpop/calceph/

bouncing or transmitting time $t_2(TDB)$ can be computed iteratively, and using this result, transmitter time $t_1(UTC)$ is also computed iteratively. The total time delay for the round-trip signal is then computed by summing the two light time solutions (up-leg and down-leg).

The procedure for modeling the spacecraft light time solution can be divided in several steps as discussed below:

2.4.2.1 Time conversion

- As discussed in the Section 2.3.1, the spacecraft observations are given in the receiver time $t_3(UTC)$. However, participants (transmitter, spacecraft, and receiver) state vectors (position and velocity) are must be computed in TDB. Thus, given receiver time $t_3(UTC)$ can be transformed into receiver time $t_3(TDB)$ as described in Section 2.4.1.

2.4.2.2 Down-leg τ_U computation

- Figure 2.12 represents the schematic diagram of the vector relationship between the participants. From this figure, the Solar system barycentric C state vector $r_3^C(t_3)$ of the Earth tracking station at receiver time $t_3(TDB)$ can be calculated by,

$$\mathrm{r_3^C(t_3) = r_E^C(t_3) \; + \; r_3^E(t_3)} \tag{2.18}$$

  where superscript and subscript are correspond to the Solar system barycenter C and the Earth geocenter E. The vector $r_E^C(t_3)$ is the state vectors of the Earth relative to Solar system barycenter C which can be obtained from the planetary ephemerides. The geocentric space-fixed state vectors $r_3^E(t_3)$ of the Earth tracking station can be calculated using proper formulation which includes Earth precession, nutation, polar motion, plate motion, ocean loading, Earth tides, and plot tide. The detail of this formulation can be find in Moyer (2003).

- The transmission time $t_2(TDB)$ and the corresponding state vectors of the spacecraft has to compute through the iterative process. In order to start the iterations, first approximation of transmission time $t_2(TDB)$ can be taken as the reception time $t_3(TDB)$. Hence, using this approximation and the geometric relationship between the vectors as shown in Figure 2.12, one can compute the spacecraft state vectors relative to the Solar system barycenter $r_2^C(t_2)$ using the spacecraft and planetary ephemerides. The approximated down-leg time delay τ_D required by the signal to reach the spacecraft from the Earth receiving station can be then computed as,

$$\mathrm{r_2^C(t_2) = \Big[r_B^C(t_2) \; + \; r_2^B(t_2) \Big]_{t_2=t_3}} \tag{2.19}$$

$$\mathrm{\tau_D \approx \frac{1}{c} \Big[\, | \, r_2^C(t_2) \; - \; r_3^C(t_3) \, | \, \Big]_{t_2=t_3}} \tag{2.20}$$

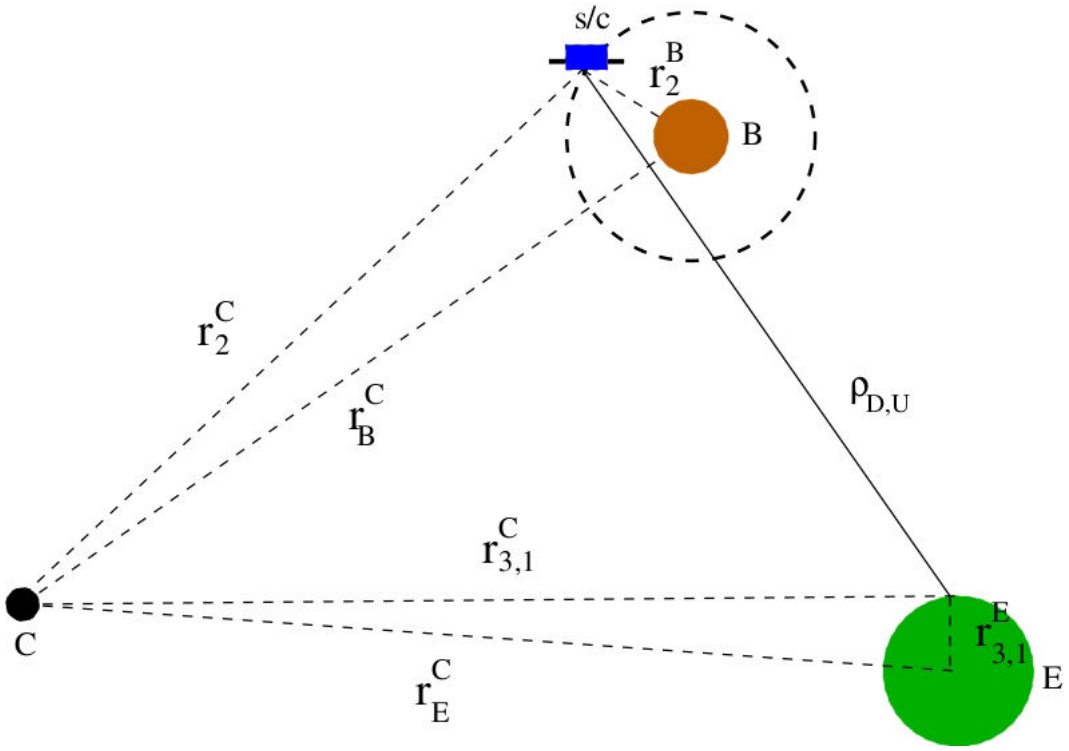

Figure 2.12: Geometric sketch of the vectors involved in the computation of the light time solution, where C is the solar system barycentric; E is the Earth geocenter; and B is the center of the central body.

where superscript B represents the central body of the orbiting spacecraft. The vector $r_B^C(t_2)$ given in Eq. 2.19 is the state vector of the central body relative to the Solar system barycenter obtained from the planetary ephemerides. While, $r_2^B(t_2)$ is the spacecraft state vectors relative to center of the central body computed from the spacecraft ephemerides. In Eq. 2.20, c is the speed of light and τ_D is the down-leg time delay which can be computed through the Eqs. 2.19 and 2.18. An estimated value of the bouncing time t_2 can be then computed as,

$$t_2 = t_3 - \tau_D \tag{2.21}$$

- Now using this result, we can then estimate the barycentric position of the spacecraft at bouncing time t_2. Hence, the down-leg vector ρ_D as shown in Figure 2.12 can be then obtained as,

$$\rho_D = r_2^C(t_2) - r_3^C(t_3) \tag{2.22}$$

The improved value of the down-leg time delay τ_D, in seconds, can be then estimated as,

$$\tau_D = \frac{1}{c}(|\rho_D|) + \delta\tau_D \tag{2.23}$$

where $\delta\tau_D$ is a down-leg light time corrections which includes the relativistic, solar corona, and media contributions to the propagation delay. Furthermore, Eqs. 2.21 to

2.23 need to iterate until the latest estimate of τ_D differs from the previous estimate by some define value such as 0.05μ.

2.4.2.3 Up-leg τ_U computation

- For round-trip light time solution, next is to compute the up-leg time delay. A similar iterative procedure as used for down-leg solution can be used the up-leg solution. Up-leg time delay τ_U which represents the time required for signal to travel between the spacecraft and the Earth transmitting station. In order to begin the iterations, first approximation can be assumed as,

$$\tau_{\mathrm{U}} \approx \tau_{\mathrm{D}} \tag{2.24}$$

Therefore, while using Eq. 2.24, approximated transmitting time $t_1(TDB)$ can be then computed as,

$$\mathrm{t_1} = \mathrm{t_2} - \tau_{\mathrm{U}} \tag{2.25}$$

- The barycentric state vectors of the transmitting station $r_1^C(t_1)$ at transmitted time $t_1(TDB)$ as shown in Figure 2.12 can be computed from Eq. 2.18 by replacing the 3 with 1, that is,

$$\mathrm{r_1^C(t_1) = r_E^C(t_1) \ + \ r_1^E(t_1)} \tag{2.26}$$

Now, using Eq. 2.26, one can compute the up-leg state vector as give by,

$$\rho_{\mathrm{U}} = \mathrm{r_2^C(t_2) \ - \ r_1^C(t_1)} \tag{2.27}$$

where $r_2^C(t_2)$ is the barycentric position of the spacecraft at bouncing time $t_2(TDB)$ and can be calculated from Eq. 2.19. Finally, the new estimation of the up-leg time delay τ_U, in seconds, is given by,

$$\tau_{\mathrm{U}} = \frac{1}{\mathrm{c}}(|\,\rho_{\mathrm{U}}\,|) + \delta\tau_{\mathrm{U}} \tag{2.28}$$

where $\delta\tau_U$ is the up-leg light time correction analogous to $\delta\tau_D$ of Eq. 2.23. Eqs. 2.25 to 2.28 are then need to iterative until the convergence is achieved.

2.4.2.4 Light time corrections, $\delta\tau_D$ and $\delta\tau_U$

2.4.2.4.1 Relativistic correction $\delta\tau_{RC}$

Electromagnetic signals that are traveling between the spacecraft and the Earth tracking encounters light time delay when it passes close to the massive celestial bodies. This effects is known as *Shapiro delay* or gravitational time delay (Shapiro, 1964). Such time delays are caused by the bending of the light path which increase the travailing path of the signal. Hence,

relativistic time delays caused by the gravitational attraction of the bodies can be expressed, in seconds, as (Shapiro, 1964; Moyer, 2003),

$$\delta\tau_{\mathrm{RC_U}} = \frac{(1+\gamma)\,\mu_{\mathrm{S}}}{\mathrm{c}^3}\,\ln\left[\frac{\mathrm{r}_1^{\mathrm{S}} + \mathrm{r}_2^{\mathrm{S}} + \mathrm{r}_{12}^{\mathrm{S}} + \frac{(1+\gamma)\,\mu_{\mathrm{S}}}{\mathrm{c}^2}}{\mathrm{r}_1^{\mathrm{S}} + \mathrm{r}_2^{\mathrm{S}} - \mathrm{r}_{12}^{\mathrm{S}} + \frac{(1+\gamma)\,\mu_{\mathrm{S}}}{\mathrm{c}^2}}\right] + \sum_{\mathrm{B}=1}^{10}\frac{(1+\gamma)\,\mu_{\mathrm{B}}}{\mathrm{c}^3}\,\ln\left[\frac{\mathrm{r}_1^{\mathrm{B}} + \mathrm{r}_2^{\mathrm{B}} + \mathrm{r}_{12}^{\mathrm{B}}}{\mathrm{r}_1^{\mathrm{S}} + \mathrm{r}_2^{\mathrm{S}} - \mathrm{r}_{12}^{\mathrm{S}}}\right] \tag{2.29}$$

where superscript S and B correspond to the Sun and the celestial body. r_1, r_2, and r_{12} are the distance between the spacecraft and the Sun S (or celestial body B), the Earth station and the Sun S (or celestial body B), and the spacecraft and the Earth station, respectively. The μ_S and μ_B are the gravitational constant of the Sun and the celestial body, respectively.

For round-trip signal, Eq. 2.29 represents the relativistic time delay $\delta\tau_{RC_U}$ relative to the up-leg of the signal. The corresponding down-leg relativistic time delay $\delta\tau_{RC_D}$ can be calculate using the same equation by replacing the 1 with 2 and 2 with 3. Hence, the total relativistic time delay, in seconds, during the round-trip of the signal can be given as,

$$\delta\tau_{\mathrm{RC}} = \delta\tau_{\mathrm{RC_U}} + \delta\tau_{\mathrm{RC_D}} \tag{2.30}$$

2.4.2.4.2 Solar Corona correction $\delta\tau_{SC}$

As mentioned in Section 2.2.3, solar corona severely degrades the radio wave signals when propagating between spacecraft and Earth tracking stations. The delay owing to the solar corona are directly proportional to the total electron contents along the LOS and inversely with the square of carrier radio wave frequency. Solar corona model for computing such delays for each legs are described in Chapter 3. The total round-trip solar corona delay, in seconds, can be written as,

$$\delta\tau_{\mathrm{SC}} = \delta\tau_{\mathrm{SC_U}} + \delta\tau_{\mathrm{SC_D}} \tag{2.31}$$

2.4.2.4.3 Media corrections $\delta\tau_{MC}$

The media corrections consist of Earth′s troposphere correction and the correction due to the charge particles of the Earth ionosphere. Such delays however relatively lesser compare to the relativistic and solar corona delays. The tropospheric model used for computing these corrections for each legs are discussed in Chao (1971); Moyer (2003). The total round-trip media correction, in seconds, can be written as,

$$\delta\tau_{\mathrm{MC}} = \delta\tau_{\mathrm{MC_U}} + \delta\tau_{\mathrm{MC_D}} \tag{2.32}$$

Figure 2.13 shows an example of relativistic correction and solar corona correction to light time solution for MGS and MESSENGER spacecraft.

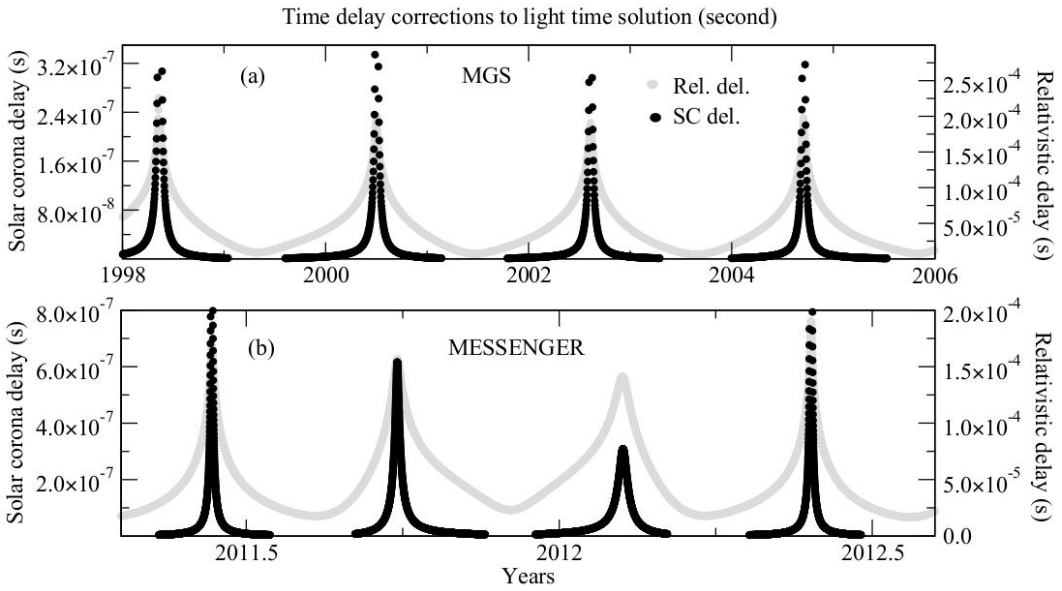

Figure 2.13: Relativistic and solar corona corrections to light time solution (expressed in seconds): (a) for MGS, (b) for MESSENGER.

2.4.2.5 Total light time delay

2.4.2.5.1 Round-trip delay

The total round-trip delay is the sum of number of terms, that includes,

$$\rho = (\tau_{\mathrm{D}} + \tau_{\mathrm{U}}) - (\mathrm{TDB} - \mathrm{TAI})_{t_3} + (\mathrm{TDB} - \mathrm{TAI})_{t_1}$$
$$-(\mathrm{TAI} - \mathrm{UTC})_{t_3} + (\mathrm{TAI} - \mathrm{UTC})_{t_1}$$
$$+\delta\rho_{\mathrm{U}} + \delta\rho_{\mathrm{D}} \tag{2.33}$$

where quantities $\delta\rho_D$ and $\delta\rho_U$ are the downlink delay at receiver and uplink delay at transmitter (see Group 3 of Section 2.3.1), respectively. The time differences given in Eq. 2.33 can be obtained as described in Section 2.4.1, while τ_D and τ_U can be obtained from Eqs. 2.23 and 2.28 respectively. Figure 2.14 illustrates an example for the total round-trip time that required by the signal to travel from the transmitter to the spacecraft (up-leg) and then from the spacecraft to the receiver (down-leg). This time solution shown in Figure 2.14 corresponds to MGS (panel *a*) and MESSENGER (panel *b*) spacecraft.

2.4.2.5.2 One-way delay

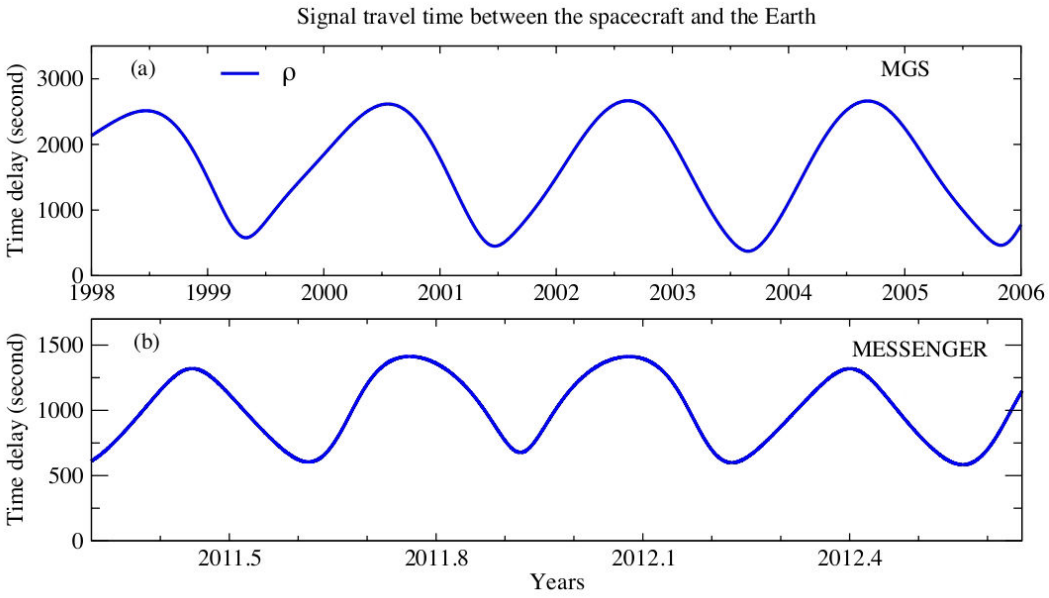

Figure 2.14: Round-trip light time solution of MGS (panel *a*) and MESSENGER (panel *b*) spacecraft, computed from the Eq. 2.33.

One-way light, in seconds, which is used to calculate the one-way Doppler observables can be calculated as,

$$\hat{\rho_1} = \rho_1 + (\text{TDB} - \text{TAI})_{t_2} \tag{2.34}$$

where ρ_1 is the difference between reception time $t_3(UTC)$ and the spacecraft transmitter time $t_2(TDB)$.

2.4.3 Doppler and range observables

The radiometric data obtained by the Earth tracking station (DSN) usually consists of three kind of measurements (one-way Doppler, two/three-way Doppler, and two-way range). The detail description of these measurements and other contents of the ODF that are useful for recognize the data are described in Section 2.3.1. Observation model which computes the observations requires the time history of the transmitted frequency at the transmitter. Such time history which contains transmitter time $t_1(UTC)$ and receiver time $t_3(UTC)$, can be obtained as described in Section 2.4.2. The corresponding transmitter frequency which can be obtained from the different forms of given frequency in ODF is described in Group 3 of Section 2.3.1.

One of the most important aspect of precise orbit determination of the spacecraft is to compute the observables. These observables require spacecraft ephemerides which can be constructed from the dynamic modeling (see Section 2.5). An observation model accounts the propagation of signal and allows to compute the frequency change between received and transmitted signal, also called *Doppler shift*. The difference between observed (given in ODF) and

computed values, also called residuals, are then used to adjust the dynamic model along with observation model for accounting the discrepancy in the models.

This section contains the formulations for computing the one-way Doppler, two/three-way Doppler, and two-way range observables. These formulations are based on Moyer (2003). The motivation for developing an observation model is to have a better understanding of the radiometric data. However, for precise computation, such as for MGS (see Chapter 3) and for MESSENGER (see Chapter 5), GINS orbit determination model (see Section 2.5) has been used. Moreover, GINS observation model is also based on Moyer (2003) formulations and the brief overview of the GINS dynamic model is described in Section 2.5.

2.4.3.1 Two-way (F_2) and Three-way (F_3) Doppler

2.4.3.1.1 Ramped

Doppler observable can be derived from the difference between the number of cycles received by a receiving station and the number of cycles produced by a fixed or ramped known reference frequency f_{REF}, during a specific count interval T_c. The given observables time-tag TT in the ODF is the mid-point of the count interval T_c (see Group 3 of Section 2.3.1). To compute these observables (Eq. 2.40), it is thus necessary to obtain the starting time $t_{3_s}(UTC)$ and the ending time $t_{3_e}(UTC)$ of the count interval, which is given in seconds by

$$\mathrm{t_{3_s}(UTC)} = \mathrm{TT} - \frac{1}{2}\,\mathrm{T_c} \tag{2.35}$$

$$\mathrm{t_{3_e}(UTC)} = \mathrm{TT} + \frac{1}{2}\,\mathrm{T_c} \tag{2.36}$$

where TT and T_c can be extracted from the ODF. Using Eqs. 2.35 and 2.36 the corresponding transmitting starting time $t_{1_s}(UTC)$ and ending time $t_{1_e}(UTC)$, in seconds, can be obtained from light time solution (see Section 2.4.2), that is,

$$\mathrm{t_{1_s}(UTC)} = \mathrm{t_{3_s}(UTC)} - \rho_\mathrm{s} \tag{2.37}$$

$$\mathrm{t_{1_e}(UTC)} = \mathrm{t_{3_e}(UTC)} - \rho_\mathrm{e} \tag{2.38}$$

where ρ_s and ρ_e is the round-trip light time computed from Eq. 2.33. Similarly, the corresponding start and end TDB at the receiving station and at the transmission station, which are required for the light time solution, can be computed as described in Section 2.4.1.

Using the time recorded history of the transmitters, the two-way Doppler F_2 and three-way Doppler F_3 can be computed as the difference in the total accumulation of the Doppler cycles, which is given as, in Hz,

$$F_{2,3} = \frac{1}{T_c}\left[\int_{t_{3_s}}^{t_{3_e}} f_{REF}(t_3)\, dt_3 \; - \int_{t_{1_s}}^{t_{1_e}} f(t_1)\, dt_1\right] \tag{2.39}$$

where $f_{REF}(t_3)$ and $f(t_1)$ can be computed from the Eqs. 2.2 and 2.3. The all time scales given in Eq. 2.39 correspond to UTC. Now by substituting Eqs. 2.2 and 2.3 into Eq. 2.39 gives, in Hz:

$$F_{2,3} = \frac{M_{2_R}}{T_c} \int_{t_{3_s}}^{t_{3_e}} f_T(t_3)\, dt_3 \; - \frac{M_2}{T_c} \int_{t_{1_s}}^{t_{1_e}} f_T(t_1)\, dt_1 \tag{2.40}$$

where M_{2_R} and M_2 are the spacecraft turnaround ratio which is given in Table 2.2. The transmitter frequency $f_T(t_1)$ at the transmitting station on Earth is ramped and can be obtained from the ramped table using Eq. 2.11. However, the transmitter frequency $f_T(t_3)$ at receiving station can be fixed or ramped. If it is ramped then it can be obtained from the ramped table using Eq. 2.11 and for fixed, Eq. 2.40 can be re-written as, in Hz:

$$F_{2,3} = M_{2_R}\, f_T(t_3) \; - \frac{M_2}{T_c} \int_{t_{1_s}}^{t_{1_e}} f_T(t_1)\, dt_1 \tag{2.41}$$

In order to compute the observables, it is necessary to solve the integrations given in Eq. 2.40. Let us assume that, W is the precision width of the interval of the integration, in seconds, which is T_c for reception interval and T_c^T for the transmission interval, and can be expressed as, in seconds:

$$T_c^T = t_{1_e} - \; t_{1_s} \tag{2.42}$$

Furthermore, let t_s be the starting time of the interval of integration which is $t_{3_s}(UTC)$ for the reception and $t_{1_s}(UTC)$ for the transmission. Similarly corresponding end time can be denoted as t_e. Each ramp of the ramp table given in the ODF is specified by the start time t_0 and end time t_f for each participating Earth stations (see Group 3 of Section 2.3.1). The interval of the integration can be covered by one or more ramps (let say n ramps). Figure 2.15 illustrates the above assumptions and the technique used for computing the integration of Eq. 2.40. In Figure 2.15, t_{start} and t_{end} is the starting and ending time of the ramp table respectively. Now using Figure 2.15 and above made assumptions, one can compute the observables as follows:

1. Compute the transmitter frequency at the start time t_s of the integration using the first ramp (see Figure 2.15) transmitter frequency. It can be achieved by using the Eq. 2.11. Therefore, the new transmitter frequency can be given as, in Hz:

$$f_0\,(t_s) = f_0\,(t_0) + \dot{f}\,(t_s - t_0) \tag{2.43}$$

   where $\dot{f}$ is the corresponding frequency rate of first ramp expressed in Hz/s.

2. If the interval of integration W contains the two or more ramp as shown in Figure 2.15, then calculates the width of each ramp i except the last ramp:

$$W_i = t_f - t_0 \tag{2.44}$$

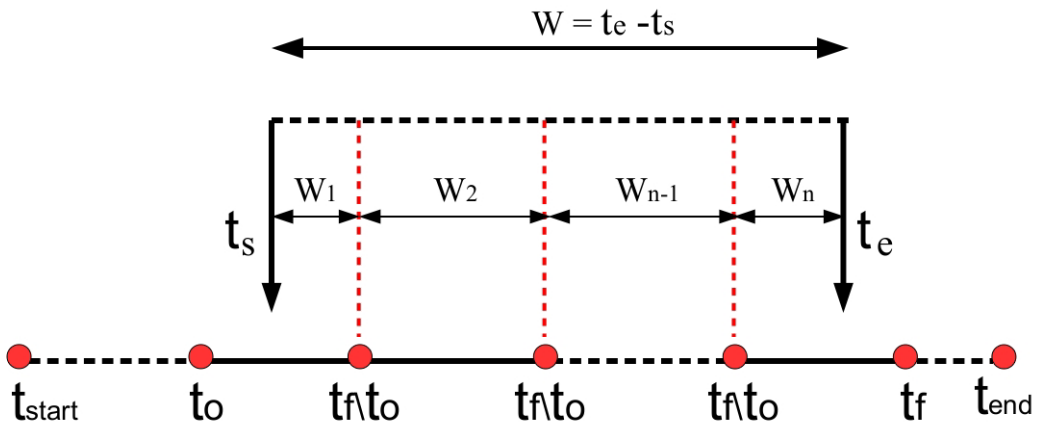

Figure 2.15: The technique used for computing the integration of Eq. 2.40. W is the precision width of the interval of the integration, and t_{start} and t_{end} is the start and end times of the ramp table (see Section 2.4.3.1).

where t_f and t_0 are the start and end times, in seconds, of each ramp (see Figure 2.15). Last ramp precision width W_n therefore computed as:

$$W_n = W - \sum_{i=1}^{n-1} W_i \tag{2.45}$$

If the interval of the integration W only contains the single ramp (n=1), then the precession width is given as:

$$W_{n=1} = W \tag{2.46}$$

3. Calculate the average of the transmitter frequency f_i for each ramp, in Hz:

$$f_i = f_0 + \frac{1}{2} \dot{f} W_i \tag{2.47}$$

where f_0 is the transmitter frequency at the each start time t_s of the ramp (see Figure 2.15) and $\dot{f}$ is the corresponding frequency rate. Ramp width W_i for each ramp can be obtained from Eq. 2.44.

4. The integral of the transmission frequency over the reception of transmission interval W can be then obtained as:

$$\int_{t_s}^{t_e} f_T(t)dt = \sum_{i=1}^{n} f_i W_i \qquad \text{cycles} \tag{2.48}$$

2.4.3.1.2 Unramped

As mentioned earlier, the given transmitter frequency can be constant or ramped. If it is constant, then it corresponds to the unramped transmitter frequency. Let us consider that, during an interval dt_1, dn cycles of the constant transmitter frequency $f_T(t_1)$ are transmitted. During the corresponding reception interval dt_3, receiving station on Earth received $M_2 dn$ cycles, where M_2 is the spacecraft turnaround ration (see Table 2.2). Therefore, the total accumulation of the constant Doppler cycles is given as, in Hz:

$$F_{2,3} = \frac{M_2\, f_T(t_1)}{T_c} \left[\int_{t_{3_s}}^{t_{3_e}} dt_3 \; - \int_{t_{1_s}}^{t_{1_e}} dt_1 \right] \tag{2.49}$$

where t_{3_s} and t_{3_e} are the start and end times of the reception time-tag TT which can be computed from Eqs. 2.35 and 2.36 respectively. Similarly t_{1_s} and t_{1_e} are the corresponding transmitting times which can be computed from Eqs. 2.37 and 2.38 respectively. All the time given in Eq. 2.49 are in UTC.

Now evaluating Eq. 2.49:

$$F_{2,3} = \frac{M_2\, f_T(t_1)}{T_c} \left\{ [t_{3_e} - t_{1_e}] - [t_{3_s} - t_{1_s}] \right\} \tag{2.50}$$

Eq. 2.50 can be used to calculate the computed values of unramped two-way F_2 and three-way F_3 Doppler observables, in Hz.

2.4.3.2 One-way (F_1) Doppler

When the radio signal is continuously transmitted from the spacecraft and received by the DSN station on Earth, then the observables are referred to one-way. These observations are always unramped and can be modeled as, in Hz, (Moyer, 2003):

$$F_1 = C_2\, f_{T_0} - \frac{1}{T_c} \int_{t_{2_s}(\mathrm{TAI})}^{t_{2_e}(\mathrm{TAI})} \left[f_T(t_2) \right] dt_2(\mathrm{TAI}) \tag{2.51}$$

where C_2 is the downlink frequency multiplier given in Table 2.3. f_{T_0} is the nominal value of spacecraft transmitter frequency $f_{S/C}$ (Eq. 2.5). $f_T(t_2)$ is the transmitter frequency at the spacecraft at transmission time $t_2(TAI)$, given by Eq. 2.4.

Now by substituting Eqs. 2.4 and 2.5 in Eq. 2.51, the one-way Doppler observables can be written as, in Hz:

$$F_1 = C_2\, f_{T_0} - \frac{C_2}{T_c} \int_{t_{2_s}(\mathrm{TAI})}^{t_{2_e}(\mathrm{TAI})} \left[f_{T_0} + \Delta f_{T_0} + f_{T_1}(t_2 - t_0) + f_{T_2}(t_2 - t_0)^2 \right] dt_2(\mathrm{TAI}) \tag{2.52}$$